OCTOBER 1975 MATT-1140

WAVE GENERATION AND HEATING NEAR ION CYCLOTRON FREQUENCY IN THE ST TOKAMAK

BY

H. TAKAHASHI

PLASMA PHYSICS LABORATORY

PRINCETON UNIVERSITY
PRINCETON, NEW JERSEY

This work was supported by U. S. Energy Research and Development Administration Contract E(11-1)-3073. Reproduction, translation, publication, use and disposal, in whole or in part, by or for the United States Government is permitted.

DISCLAIMER

NOTICE

Printed in the United States of America.

Available from
National Technical Information Service
U. S. Department of Commerce
5285 Port Royal Road
Springfield, Virginia 22151
Price: Printed Copy $ * ; Microfiche $1.45

*Pages	NTIS Selling Price
1-50	$ 4.00
51-150	5.45
151-325	7.60
326-500	10.60
501-1000	13.60

Wave Generation and Heating Near Ion Cyclotron Frequency in the ST Tokamak*

H. Takahashi
Plasma Physics Laboratory, Princeton University,
Princeton, New Jersey 08540

ABSTRACT

The results of the recent, high power ICRH experiments performed on the ST Tokamak are reported. It was demonstrated that both the fast and slow waves could be generated in toroidal geometry, and heating of the plasma ions at power levels up to 1 MW was observed both at the ion cyclotron frequency (ω_{ci}) and its second harmonic ($2\omega_{ci}$). Measurements by a charge exchange neutral detector directed tangentially to the plasma torus revealed that at $2\omega_{ci}$ the ion energy within the bulk of the ion distribution function ("parallel body temperature") could be increased from about 100 eV up to 200 eV with efficiencies ranging from 8 to 45%. Efficiency at ω_{ci} in raising the parallel temperature was less than at $2\omega_{ci}$. Charge exchange neutral detection perpendicular to the plasma column showed that both at ω_{ci} and $2\omega_{ci}$ the "perpendicular body temperature" was enhanced very rapidly by a factor of up to 3. Also, buildup of a high energy "tail" in the ion energy distribution was observed. Power transfer to the ions seemed extremely efficient. However, in the present experiment, the maximum attainable ion temperature increase was limited by rapid loss of high energy ions, presumably through particle orbit loss cones. Some experimental evidence

for the loss mechanism is presented. The problem was particularly severe in the present experiments because the low frequency (25 MHz) of the available generator forced operation of the device with field and current too low to attain good confinement. The principal limitations on the maximum energy input resulted from disruptive instabilities following influx of neutrals from the limiters and walls. Some indications that this was caused by sputtering by resonantly accelerated oxygen ions were observed. Appearance of toroidal eigenmodes as sharp peaks in the loading resistance was also observed. Extrapolation to larger tokamaks of the coming generation supports a bright outlook for the rf heating in this frequency range.

*The content of this report was presented as invited paper 8A-1,2,3 at the 16th Annual Meeting of the Div. of Plasma Physics, APS, Albuquerque, N. M., 28-31 October, 1974.

INTRODUCTION

We have conducted experiments in the ST Tokamak on plasma heating by the fast wave at the second harmonic of the ion cyclotron frequency and by the ion cyclotron wave at the fundamental resonant frequency. We call these experiments simply ICRH experiments. This paper summarizes the work[9] conducted by the following team of researchers:

J. Adam
H. Eubank
W. Getty
E. Hinnov
W. Hooke
J. Hosea
F. Jobes
R. Sinclair
H. Takahashi

This summary concerns primarily the ion heating aspects of the experiments[10] and also contains the results of further analyses of the experimental data beyond those presented elsewhere.[9]

From earlier experiences with the C. Stellarator[1] and many other devices, it had been known that ICRH is an efficient method of heating plasma ions. However, before these earlier successful results in essentially linear geometries are translated to toroidal geometries and larger scale experiments on a tokamak are attempted, certain questions had to be answered: For example, can wave generation and propagation take place in the inhomogeneous magnetic field of a tokamak, and can ion heating take place in the absence of magnetic beaches? The present series of experiments were designed to provide answers to these questions. Earlier, we have reported[2] the results of lower power experiments designed primarily to study wave generation. The emphasis of our recent efforts lie in high power ion heating and this presentation is accordingly centered around this aspect. However, a few important findings on wave generation will also be touched upon.

Our experimental set-up is shown schematically in Fig. 1. This is the plan view of the ST Tokamak showing the plasma torus and an array of toroidal field coils. For the heating experiments the device was operated most of the time at a toroidal field of 16 kG and an Ohmic heating current of 25 kA. With this discharge the line average electron density was between o.6 and 1.2 $\times 10^{13}$ cm^{-3} and the peak electron temperature was about 650 eV. The ion temperature without rf heating was less than 100 eV, this was a rather feeble discharge compared to what the machine was capable of producing. These operating conditions were forced upon us by the 25 MHz frequency of the available generator, requiring a low toroidal field (16 kG) for the second harmonic of the deuteron cyclotron frequency, and a scaled down Ohmic heating current to maintain a stable discharge. As we shall see below, this resulted in poor confinement of heated ions.

The waves were generated by a pair of half-turn rf coils shown in Fig. 1. The means of assessing ion heating were two charge exchange neutral atom detectors. One of them was located near the rf coil looking perpendicularly at the plasma torus, and the other on the far side looking tangentially. Since the latter is on the side of the torus opposite the rf coils, it is reasonable to assume that the entire plasma is heated to a temperature at least as high as the temperature indicated by this detector. The measurement by this detector is the one we use in assessing ion heating.

In Fig. 2 the minor cross section of the plasma and one of the half-turn coils that run in the inner side of the torus are shown. The toroidal magnetic field falls off as a function of

increasing major radius. By changing the toroidal field strength we can place this resonant layer where we wish. The quantity Ω that appears often in later discussions is defined as $\Omega = \omega/\omega_{ci}$. $\Omega = 1$ and $\Omega = 2$ are therefore the fundamental and the second harmonic resonance conditions.

METHOD OF EVALUATING ION HEATING

Figure 3 shows what happens to the charge exchange neutral signal when a rf pulse is applied. The abscissa is the setting of the energy analyzer, and the ordinate is the logarithm of the detector signal divided by a known function of the energy. The curves have been displaced vertically for better visibility. Time is measured from the start of the rf pulse. Each of these points represents the average of three shots. If the particle energy distribution is Maxwellian, these points should lie on a straight line and the reciprocal of its slope gives the temperature.

The left-hand figure refers to the perpendicular detector. Starting from a Maxwellian distribution before the application of the rf pulse, we see that a huge "tail" is formed shortly after the initiation of the pulse, this tail formation is also predicted theoretically.[8] As time elapses, the distribution is seen to relax closer toward a Maxwellian. Similar behavior is also observed for the tangential detector but the tail formation is less pronounced. We are dealing with essentially non-Maxwellian energy distributions, but we wish to characterize heating effect by some convenient parameter like temperature. To do this we fit two straight lines to these data points as

shown in Fig. 4. We call the effective temperature determined from the low energy part of the distribution the "body" temperature, and the one from the high energy part the "tail" temperature. All subsequent references to ion temperatures are, unless otherwise specified, these body temperatures. Therefore, we are being conservative in assessing the energy content of the measured part of the distribution function.

ION HEATING

Let us now look at the ion heating results. Figure 5 shows how the perpendicular temperature varies with time as the $\Omega = 2$ plane is moved across the plasma column. Going clockwise from the left-top figure, Fig. 5 (a)-(c), we see that the temperature increase is largest when the resonant plane is positioned at the center. The last figure [Fig. 5(d)] shows a result that is intriguing at first sight: some heating was observed even when the resonant plane was completely outside the plasma. We attribute this to resonant heating of impurity ions, and subsequent transfer of energy to deuterons by collisions, the $\Omega = 2$ resonant planes of O^{7+} and O^{6+} were still inside the plasma. We shall have more to say about the effect of impurity ions on heating and sputtering.

Figures 5(a) and (b) have the $\Omega_{D+} = 2$ resonant layer at R = 104 cm and R = 110 cm respectively. The third (c) case has $\Omega_{D+} = 2$ at R = 118 cm and $\Omega_{O}7+ = 2$ at R = 103 cm. The fourth (d) case has $\Omega_{D+} = 2$ at R = 131 cm, $\Omega_{O}7+ = 2$ at R = 115 cm and $\Omega_{O}6+ = 2$ at R = 99 cm. Wave power is about 76 kW except for the third (c) case with 89 kW.

The smaller second peak in the temperature appearing at about 9 msec after the beginning of the rf pulse is caused by the influx of high-Z impurities from the walls and limiters. The high-Z impurities increase the electron-ion coupling and make Ohmic heating more effective. In fact the electron-ion equi-partition time for these cases is about 9 msec. [This impurity heating effect must not be confused with heating due to resonant acceleration of oxygen ions mentioned in connection to Fig. 5(d).]

> The effective Z determined from the resistivity rises from 2.9 to 3.9 due to high-Z impurities released by rf pulse. The electron-ion equi-partition time is given by (Spitzer, p. 135) t_{eq} (msec) = 994 (A/Z^2) $T_e^{3/2}$ (keV)/n_e (10^{13} cm^{-3}) $\ln\Lambda$. This gives t_{eq} = 9.13 msec for T_e = 0.65 keV, Z = 3.9, $n_e = 0.5 \times 10^{13}$ and $\ln\Lambda \simeq 15$. The temperature drops again after the second peak, presumably because the Ohmic discharge returns to the original equilibrium state.

For all the ion temperature results presented here, the rf pulse length is only about 1 msec long and the rf and high-Z impurity heating effects were well separated from each other. In the subsequent discussions only the temperature increase due to rf heating is considered.

Some cases of the parallel temperature response are shown in Fig. 6. Through cyclotron resonance the ions gain energy from the wave field in the perpendicular degrees of freedom, and through Coulomb collisions the energy spreads into the parallel degree of freedom. $T_\parallel$ rises therefore more slowly than $T_\perp$ as is evident from the figure.

As indicated in the figure, we have observed the appearance of disruptive instabilities when the energy input into the plasma exceeded several hundred Joules. Since the ion energy confinement

time (computed for parabolic radial density and temperature profiles) was about 4 msec for these cases, the optimum rf pulse length would have been greater than 4 msec. However, the disruptive instabilities caused by the impurity influx and subsequent narrowing of the current channel prevented the use of rf pulses longer than 1-2 msec. This was one of the processes that limited the maximum attainable heating and will be discussed later in more detail.

The previous results refer to $\Omega = 2$ heating. Measurements at $\Omega = 1$ show a smaller increase in $T_{\parallel}$, although the increase in $T_{\perp}$ was comparable to $\Omega = 2$ heating. It was also observed that unlike the fast wave ($\Omega = 2$) the ion cyclotron waves ($\Omega = 1$) did not propagate around the torus. Heating was accordingly localized near the coil and the parallel temperature detector on the far side of the torus indicated only small temperature changes. It must also be noted here that, because of the impurity problems, nearly all of the heating experiments at the fundamental cyclotron frequency were conducted with the resonant layer positioned near the outer edge of the plasma resulting in poorer confinement of the heated ions.

For the data presented in Fig. 6, the line average electron density varied from $0.6 \sim 1.2 \times 10^{13}$ cm^{-3}, the net rf power in the wave field varied from 75 ~ 150 kW, except for the top left [Fig. 6(a)] case with 350 kW, and the pulse length ranged from 0.6 ~ 1.7 msec. Various normalizations were applied to these data in order to facilitate comparisons, shown in Fig. 7.

Figure 7(a) shows the increase in $T_{\parallel}$ due to rf heating ranging from 40 eV to 110 eV. The abscissa is the power times

the pulse length divided by the total number of ions in the machine. This quantity represents the amount of energy available for heating, expressed in units of keV per ion. The curve tends to saturate as the available energy per ion increases indicating decreasing efficiency. The reason for this falling efficiency will be discussed below. In order to have some idea as to where our present achievement stands relative to alternative means of supplementary heating, we have also plotted the latest results from the neutral beam injection heating experiments[3] conducted in the ATC machine. The temperature rise attributable to injection is plotted against similarly defined available heating energy per ion. The beam pulse length is 10 msec in these experiments and the Ohmic heating current is between 60 and 70 kA, compared to 25 kA for the ST experiments. Multiplying ΔT by $3/2\ k$ we obtain the ion energy increase per ion. Dividing this quantity by the available heating energy gives an efficiency which is plotted in Fig. 7(b). This efficiency based upon the total temperature rise ranges from 8% to 45% for the present ICRH experiments.

Alternatively, we may define a heating rate efficiency based on the power input into the ions which is plotted in Fig. 7(c). The power input was normalized to account for different densities. For neutral beam injection the heating rate was greatest during the first 1 msec of the pulse. It is this higher rate that is used in Fig. 7(c). In all of these experiments, we see that the results of the two alternative methods of heating are comparable. We must keep in mind,

however, these experiments were carried out in two different devices with different plasma properties. In particular, confinement properties of the ATC plasma were superior to those of the ST plasma under present experimental conditions.

We now leave the description of the experiments and their results and discuss the principal difficulties encountered in our quest for higher ΔT_i. There are two tasks: one is to identify the principal cause of power loss and account for the falling efficiencies with increasing energy input and the other to explain the neutral gas influx that led to disruptive instabilities.

LOSS OF ENERGETIC IONS THROUGH LOSS CONES

We believe that the dominant mechanism of energy loss in the present experiments was the loss of energetic ions through particle orbit loss cones. In Fig. 8 the loss cones for the ST Tokamak under the present operating conditions are sketched in the customary manner. (Loss cones shown in Figs. 8 and 9 are presented in the manner originally due to J. Rome[7] and these specific results were obtained using a computer code prepared by R. Smith.)

> For several radial positions associated loss cones are shown in the $E_\perp$ - $E_\parallel$ energy space. The negative value of $E_\parallel$ refers to ions moving against the Ohmic heating current. If an ion located at a radial position, e.g., at r/a = 0.6, happens to possess energy above and to the left of the associates loss-cone curve, then it is on a drift orbit too large to be contained within the plasma and ends up striking a limiter or the vacuum vessel wall. Ions with energies below and to the right of this curve are contained.

Note that the loss cones extend down almost to the thermal energy indicated by a shaded triangular region near the origin. Most ions are originally contained within this region. The wave field accelerates ions in the perpendicular directions and the distribution becomes stretched in the vertical direction.

> If we imagine the third coordinate axis perpendicular to the plane of the paper representing the distribution function, the original isotropic distribution is represented by contour lines running at 45° with respect to the horizontal axis as shown near the origin. In the process of heating, ions moving along field lines pass through the thin resonant layer many times with their initial phase randomized by Coulomb collisions. Therefore the resonant heating in the present situations is a diffusive process in velocity space.[8] But the resonant acceleration is in the perpendicular directions and the distribution becomes enormously elongated in the vertical direction upon application of an rf pulse.

Most of the ions with large values of $E_\perp$ are trapped in banana orbits. (The trajectory in the energy space of a portion of the banana orbit is illustrated in the figure by a 45° line segment starting at $E_\perp$ = 2 keV.) These ions are either on uncontained banana orbits and are on their way out of the plasma, or they are on contained orbits but are likely to be pitch-angle scattered onto uncontained orbits by small Coulomb collisions within a fraction of the deflection time. Clearly, the lifetime of these ions is of the order of the bounce time around the banana orbit and a large amount of power could be lost from the plasma by these processes.[6]

Experimental evidence that these processes were indeed taking place in our experiment is provided by charge exchange neutral signals in Fig. 8. The top oscillogram is from the

perpendicular detector and the bottom is from the tangential detector. The perpendicular signal rises quite sharply indicating high effectiveness of the wave field in accelerating the ions. But the signal comes quickly to a saturation level suggesting existence of some strong loss mechanisms. On the other hand, the parallel signal increases more gradually over the entire period of the rf pulse. Notice also that the perpendicular signal is an order of magnitude greater than the parallel signal at the same energy. Considering the difference in the length of the line of sight the perpendicular signal intensity is nearly 50 times the parallel signal intensity. This is evidence of a strongly anisotropic distribution.

Now, for the effects of the loss cones let us look at the relaxation process following the termination of the rf pulse. Starting from a highly anisotropic state, the ion distribution relaxes toward a more isotropic state through deflecting collisions that alter the direction of the motion of an ion but keep its energy essentially unaltered. In the absence of the loss cones, the amplitude of the distribution function along the parallel energy axis should build up at the expense of the amplitude along the perpendicular axis.

> More precisely, particle depletion from the energy range under observation due to the slowing-down process competes with the particle influx due to the deflection process. However, at high energies, the deflection is a faster process than the slowing-down. The trajectory in energy space of an ion undergoing such deflection is illustrated in Fig. 8 by a 45° line through the point A. The process is again diffusion in velocity space and ions carry out random walks along such trajectories,

but the net effect of the isotropizing relaxation processes is the downward migration of ions. Trapped ions would move onto larger banana orbits and become eventually circulating ions.

Clearly, the signal from the parallel detector must increase, rather than decrease, after the end of the rf pulse at the expense of the decreasing signal from the perpendicular detector. A glance at the oscillograms in the figure shows that the observed $E_{\parallel}$ signal decreased in contrast to these expectations. The explanation is that, because of intervening loss cones, this direct isotropization path was closed to most of the energetic ions and they escape via the loss cones. The decay time of the perpendicular signal is a measure of the time scale within which these ions are lost. As the power input and hence the wave amplitude increases, ions are accelerated to higher perpendicular energies resulting in greater energy loss. This picture is consistent with the observed decrease of heating efficiency as the power input was increased.

Quantitatively speaking, we are trying to account for the fate of the rf power ranging from several tens of kW to a few hundred kW that went into the rf field but did not appear as an increase in $T_{\parallel}$. Now, according to our two Maxwellian representation of the ion distribution, the tail of the distribution contains approximately between 8% and 40% of the total ion energy. This energy is lost on a time scale comparable to the decay time of the $E_{\perp}$ signal. From this, we estimate roughly that some 20 to 200 kW of the power loss could be accounted for by this loss cone mechanism.

It must be emphasized at this point, however, that this large power loss due to loss cones was caused by the unusually low Ohmic heating current with which we had to operate the device. To make this point clear, Fig. 9 compares the loss cones of ST under the present operating conditions and those of ATC under which the neutral beam injection experiments were performed. Far superior confinement capabilities of the ATC plasma are evident from this figure. The loss cones in future larger devices such as PLT and T10 lie in much higher energy ranges and their influence will be greatly reduced.

IMPURITY INFLUX

When the total energy input from ICRH exceeded several hundred Joules, we encountered another difficulty; the plasma became unstable due to impurity influx. Figure 10 shows the sequence of events leading to disruptive instabilities when the rf power was applied for a prolonged period. Thomson scattering radial profiles of the electron density showed the density increase first appeared at the edge of the plasma and then moved inward. The electrons were cooled near the edge while they were heated at the center leading to an increasingly narrower current channel. The incremental density increase was strongly dependent on machine conditions. It became progressively smaller as the machine became cleaner and as the base pressure decreased toward the end of the experimental period. As the density increased, the loop voltage rose and finally led to disruptive instabilities and characteristic negative voltage spikes appeared.

Figure 11 shows how the incremental density increase due to a 2.5 msec rf pulse varied with the confining field currents. The values of the current for the $\Omega = 2$ and $\Omega = 1$ deuteron resonant layers to be located at the center of the plasma are indicated along the abscissa. We naturally suspected that the impurity influx was caused by bombardment by energetic deuterons that escaped through the loss cones. However, the dependence shown here is inconsistent with the picture of deuteron bombardment alone. The maximum was not located at the deuteron resonances but was between the two deuteron resonances. The $\Omega = 2$ condition corresponds to a minimum and the increment at $\Omega = 1$ was much greater than that at $\Omega = 2$. When we also indicate on the same plot the resonance layers of various oxygen ions, the picture became clearer. Although impurity oxygen ion concentration was at most a few percent (an effective-Z measurement indicated oxygen concentration of 3% before rf and 5% after rf, while spectroscopic measurements gave increase of the concentration from 2% to 4% due to the rf pulse), the sputtering efficiency of impurity ion scales as Z^2M and, therefore, an O^{5+} ion has a sputtering yield 200 times that of a deuteron at the same energy. We see from the figure that O^{6+} and O^{5+} ions were probably responsible for the central maximum, while the peak at $\Omega = 1$ was probably caused by O^{4+} as well as deuterons. These ions with low ionization potentials would be concentrated near the edge of the plasma where the confinement is poor. On the other hand, O^{7+} and O^{8+} with much higher ionization potentials would be concentrated near the axis where T_e was high, they were, therefore, better contained and were probably contributing to heating rather than sputtering. It

should be added here that these multiply charged oxygen ions are resonantly accelerated as effectively as deuterons by the rf field,[6] and hence become as energetic as the deuterons.

> Multiply stripped metal ions such as iron and molybdenum can also be resonantly accelerated. But these do not seem to be the source of sputtering in the present case: the successive cyclotron resonances of these ions are finely spaced and hence, if these ions were responsible for sputtering, the "dip" in the density increase curve of Fig. 11 between $\Omega_o 4^+ = 2$ and $\Omega_o 5^+ = 2$ resonances could not be explained. Further, the electron temperature was too low to multiply ionize significant number of these heavy ions. If the resonant acceleration and expulsion through loss cones of impurity ions was indeed what was happening in these experiments, it is not unreasonable to think of exploiting such phenomena to rid the plasma of impurity ions. This is analogous to a scheme proposed by Samain,[5] in which the resonant acceleration is utilized to trap impurity ions within magnetic field ripples. The trapped ions leave the plasma due to unsymmetric drift as they bounce between the local mirrors.

We now come to the question of whether the rf field itself was the cause of instabilities. There are strong indications that this was not the case. For example, we observed that the instabilities occurred well after the rf pulse had ended, and we could simulate the processes leading to instabilities by injecting cold gas into the vacuum vessel through a pulsed gas valve. This experiment also showed that injection of deuterium gas had no effect on the plasma stability or the ion temperature, while injection of heavy gases such as N_e and N_2 caused disruptive instabilities to occur and the ion temperature to rise. We conclude that heavy impurities, but not the recycled deuterium, were primarily responsible for the disruptive instabilities.[9]

TOROIDAL EIGENMODE TRACKING

We now turn our attention to one aspect of wave generation in a toroidal geometry. There will be a more detailed report on this subject by W. Getty and Hosea[11] later in this session, but we wish to mention one finding which we believe must be considered in assessing future prospect of ICRH.

One way to characterize wave generation efficiency is to represent the loading of the generating circuit due to radiation of the waves by an equivalent series resistance. This resistance is computed by dividing the net power input into the coil by the square of the coil current. Figure 13(a) shows the time variation of the series resistance at the fixed magnetic field corresponding to $\Omega = 1.16$ at the center of the plasma. As the Ohmic discharge evolves the electron density varies as shown in Fig. 13(b). This density variation causes the loading of the circuit also to vary with time. The greater the loading resistance, the greater the fraction of the power that goes into the wave compared to the circuit loss. We interpret sharp peaks in the loading curve as appearance of toroidal eigenmodes.[4] Under these conditions the vacuum vessel is acting as a plasma-filled toroidal cavity at a resonance. If we can excite one of these eigenmodes and then stay on top of it as the plasma condition evolves with time by suitable means, e.g., by feedback control, we could greatly enhance the wave generation efficiency and circuit loss would be negligible. This would also have a desirable consequence of reduced voltage across the coil for a given rf power, thus ameliorating the voltage breakdown problem - often a bottleneck in the high power rf heating experiments.

SUMMARY AND FUTURE PROSPECTS

We have demonstrated through these experiments that the ions in a Tokamak can be heated by ICRH. Its effectiveness in terms of incremental temperature rise as well as efficiency is comparable to the achievement of the neutral beam injection heating conducted in ATC.

The major source of power losses was identified as the loss-cone loss, which was really a peculiarity of the present experiment rather than something inherent to ICRH itself. We can reasonably extrapolate the present results to an experiment under more optimum conditions, especially in larger devices such as PLT, T10, etc. in which loss cones pose much less problems, and expect greatly improved heating efficiencies. Exploitation of toroidal cavity resonance should also greatly enhance the wave generating efficiency and ameliorate the voltage breakdown problems. In these regards ICRH appears to be a very attractive means of heating ions in the coming generation of Tokamaks.

On the other hand, indications of a new, potentially troublesome source of difficulties, i.e., resonant acceleration of impurity ions and consequent sputtering of heavy impurities was observed. Well coordinated efforts to minimize the influence of impurities may become necessary in the future experiments.

Theoretical analysis of toroidal eigenmodes and heating rate in inhomogeneous bounded plasma will be helpful for designing future experiments. Experimentally, a test of heating efficiency under the optimized conditions, without being penalized by poor

confinement of heated ions, is called for. Influence of resonant acceleration of impurity ions must be studied more extensively. Solving some technological problems associated with toroidal mode tracking at large power levels is also needed.

ACKNOWLEDGMENTS

In preparation of this paper, the author was greatly benefited from discussions with and suggestions from F. Perkins, T. Stix, J. Sinnis, S. von Goeler, R. Smith, S. Cohen and E. Meservey. In particular the author is grateful to F. Perkins for bringing to the author's attention a work by J. Rome on loss cones for neutral beam injection and for suggesting that a similar mechanism might be responsible for the power loss in the present experiments.

This work was supported by United States Energy Research and Development Administration Contract E(11-1)-3073.

REFERENCES

[1]M. A. ROTHMAN, et al., Phys. Fluids 12 (1969) 2211.

[2]J. C. HOSEA and W. M. HOOKE, Phys. Rev. Lett. 31 (1973) 150.

[3]H. P. EUBANK, Symposium on Plasma Heating and Injection, Varenna, Italy (1974).

[4]F. W. PERKINS, et al., Third International Symposium on Toroidal Plasma, Garching, Germany (1973) paper B-8.

[5]A. SAMAIN, Symposium on Plasma Heating in Toroidal Devices, Varenna, Italy (September, 1974).

[6]F. W. PERKINS, private communication.

[7]J. A. ROME, et al., Meeting on Theoretical Aspects of CTR, Berkeley, (April 4, 1974).

[8]F. W. PERKINS, Paper 8A5, and T. H. STIX, Paper 8A8, The Sixteenth Annual Meeting of the Div. of Plasma Physics, APS, Albuquerque, N. M., 28-31 (October, 1974).

[9]The paper, IAEA-CN-33/A3-2, by J. ADAM, et al. was submitted to the International Conference on Plasma Physics and Controlled Thermonuclear Fusion Research, Tokyo, Japan (November, 1974).

[10]More details on the wave propagation aspects of the experiments may be found in the paper by J. HOSEA, Symposium on Plasma Heating in Toroidal Devices, Varenna, Italy (September, 1974).

[11]W. D. GETTY and J. C. HOSEA, The Sixteenth Annual Meeting of the Div. of Plasma Physics, APS, Alberquerque, N. M., 28-31, (October, 1974) Paper 8A6.

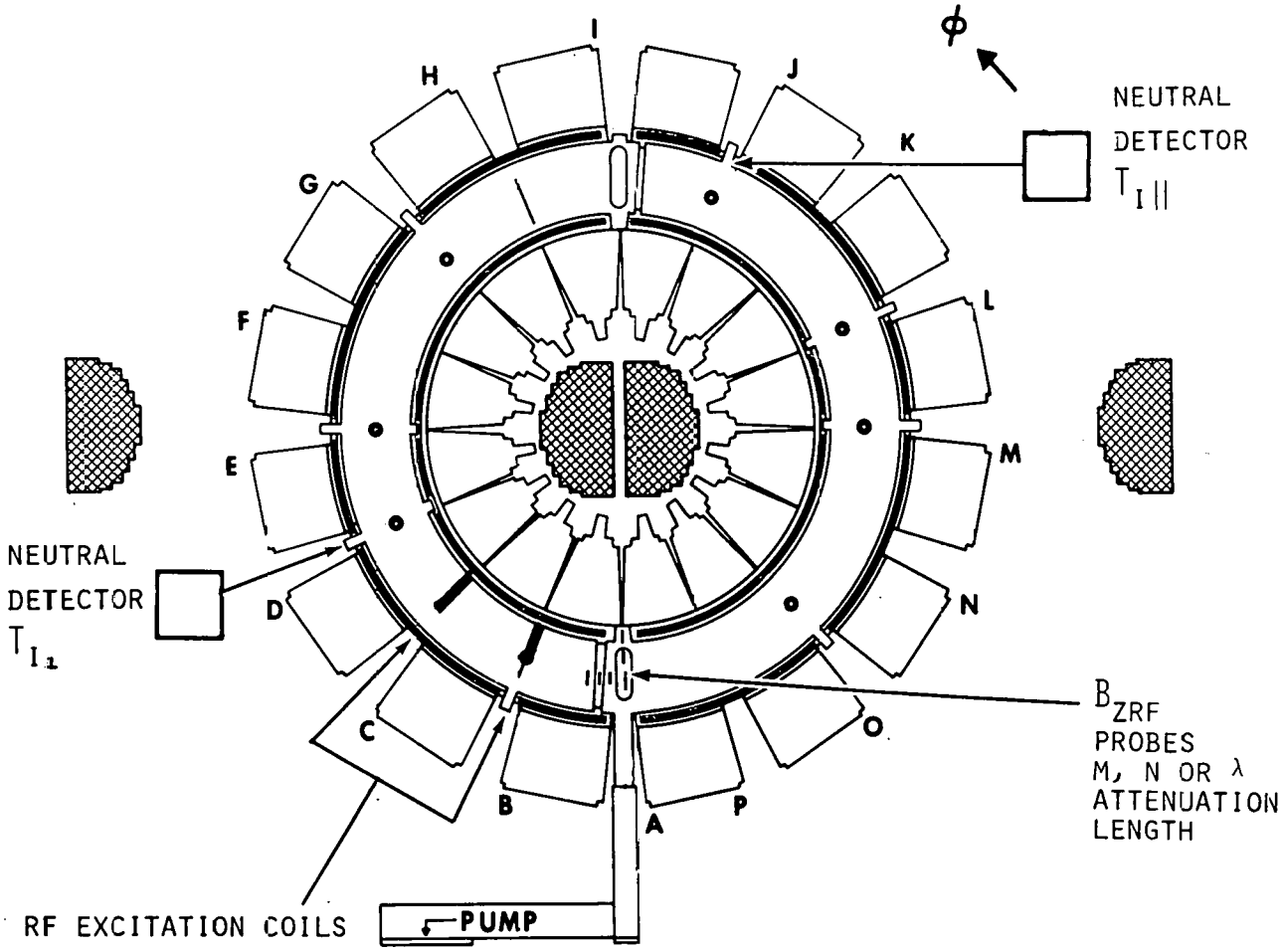

$$\left[F_{RF},\ I_{RF},\ V_{RF}:\ R_S = P_{RF}/I_{RF}^2\ ,\ R_P = \frac{V_{RF}^2}{P_{RF}}\right]$$

743866

Fig. 1. Plan view of the ST Tokamak. Locations of two half-turn rf coils and two charge-exchange neutral detectors are indicated.

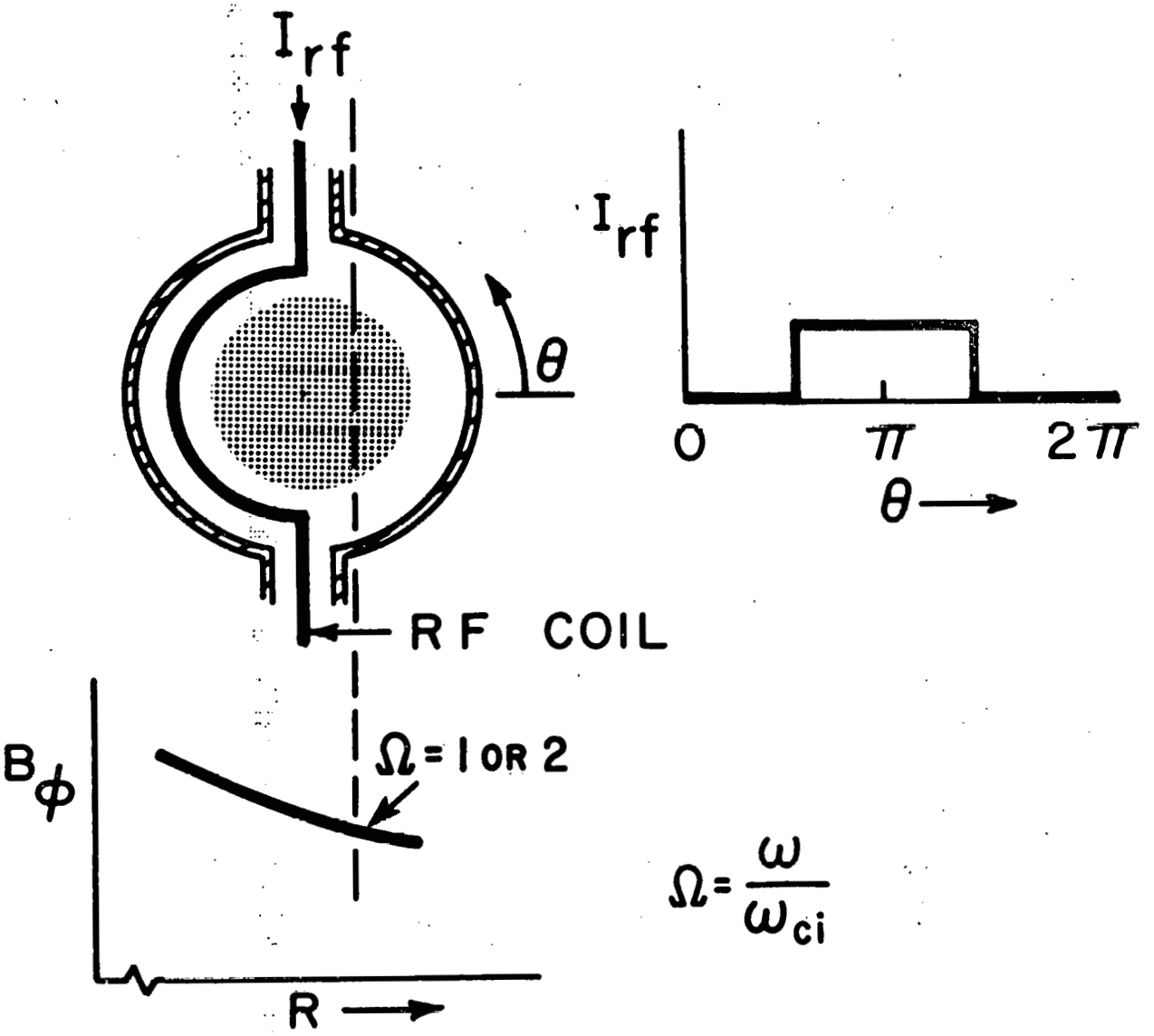

743865

Fig. 2. Minor cross section of the plasma and a half-turn rf coil. Toroidal magnetic field falls off as a function of increasing major radius and the cyclotron resonance condition is satisfied on a cylindrical surface of constant major radius.

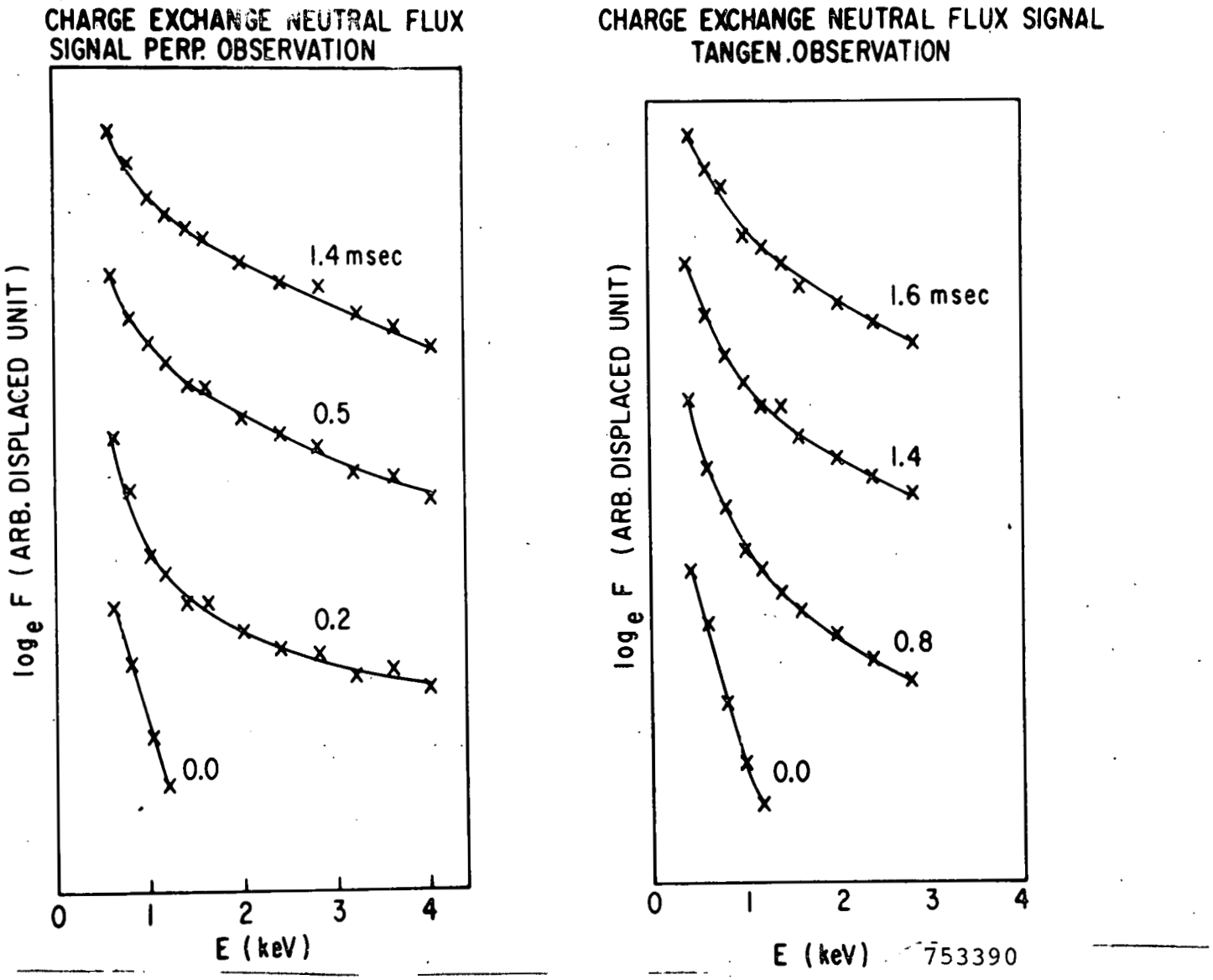

Fig. 3. Evolution of the perpendicular and parallel ion energy distributions. F is the signal intensity from the charge exchange neutral detectors divided by a known function of the energy analyzer setting. RF pulse is turned on at $t = 0$. Curves are displaced vertically for better visibility.

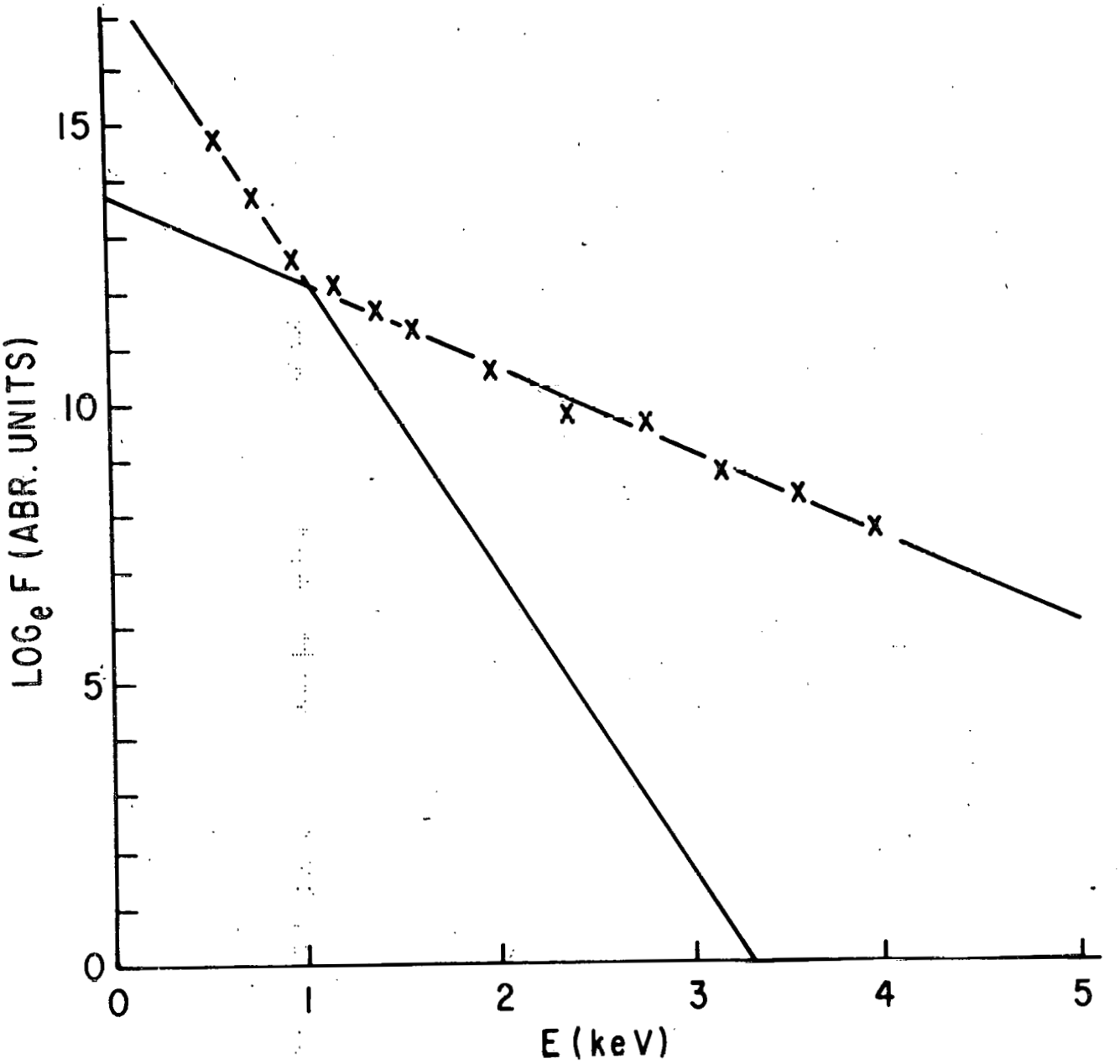

753218

Fig. 4. Two-Maxwellian representation of the measured distribution function. The reciprocal of the slope of the two straight lines give temperatures. The "body" temperature determined from the low energy part of the distribution is used to assess ion heating.

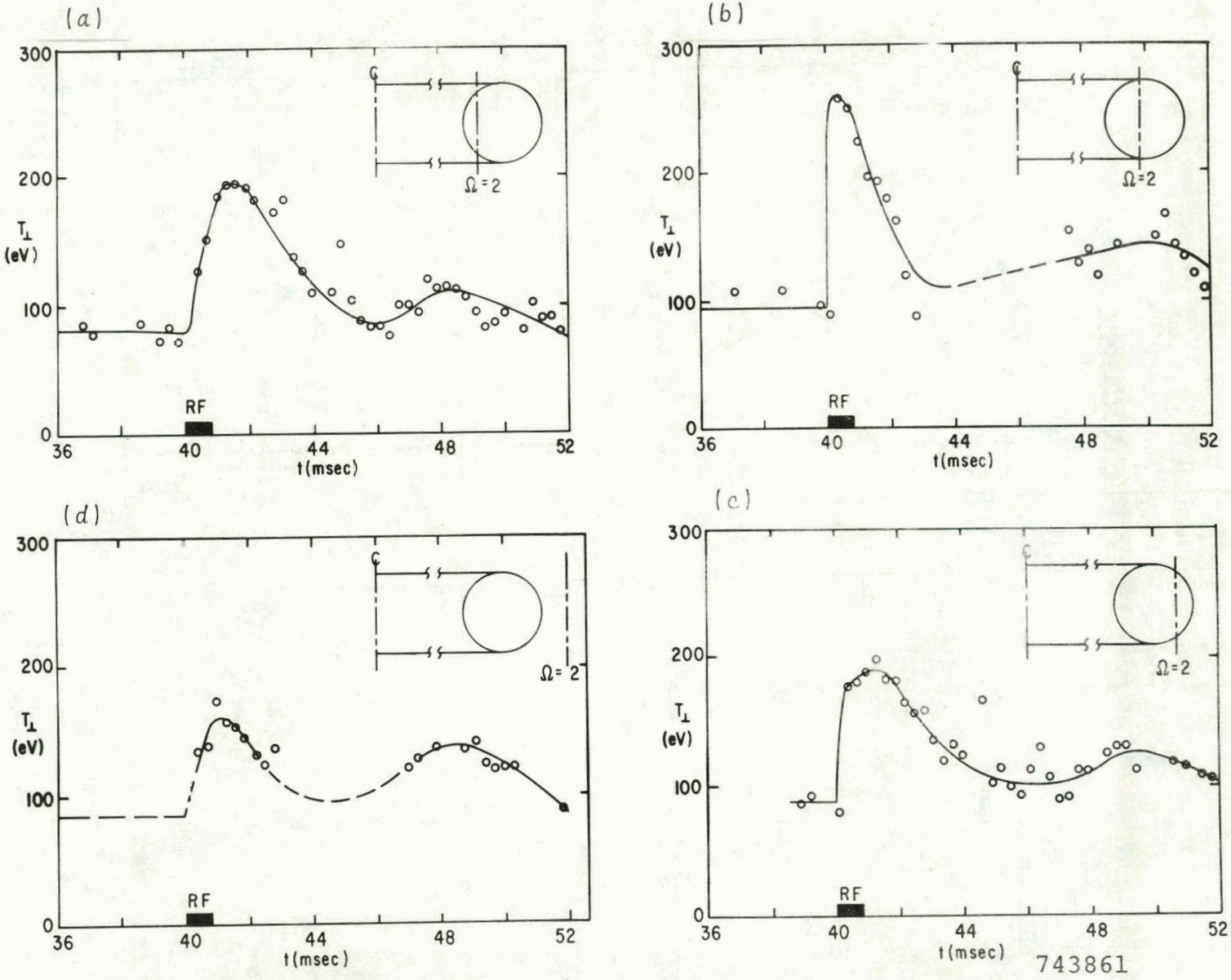

Fig. 5. Perpendicular temperature response as the $\Omega = 2$ deuteron resonant plane moves across the plasma column. Heating in the case d, for which the resonant plane for deuterons is completely outside the plasma, is attributed to resonant heating of oxygen ions, and subsequent energy transfer to deuterons through collisions.

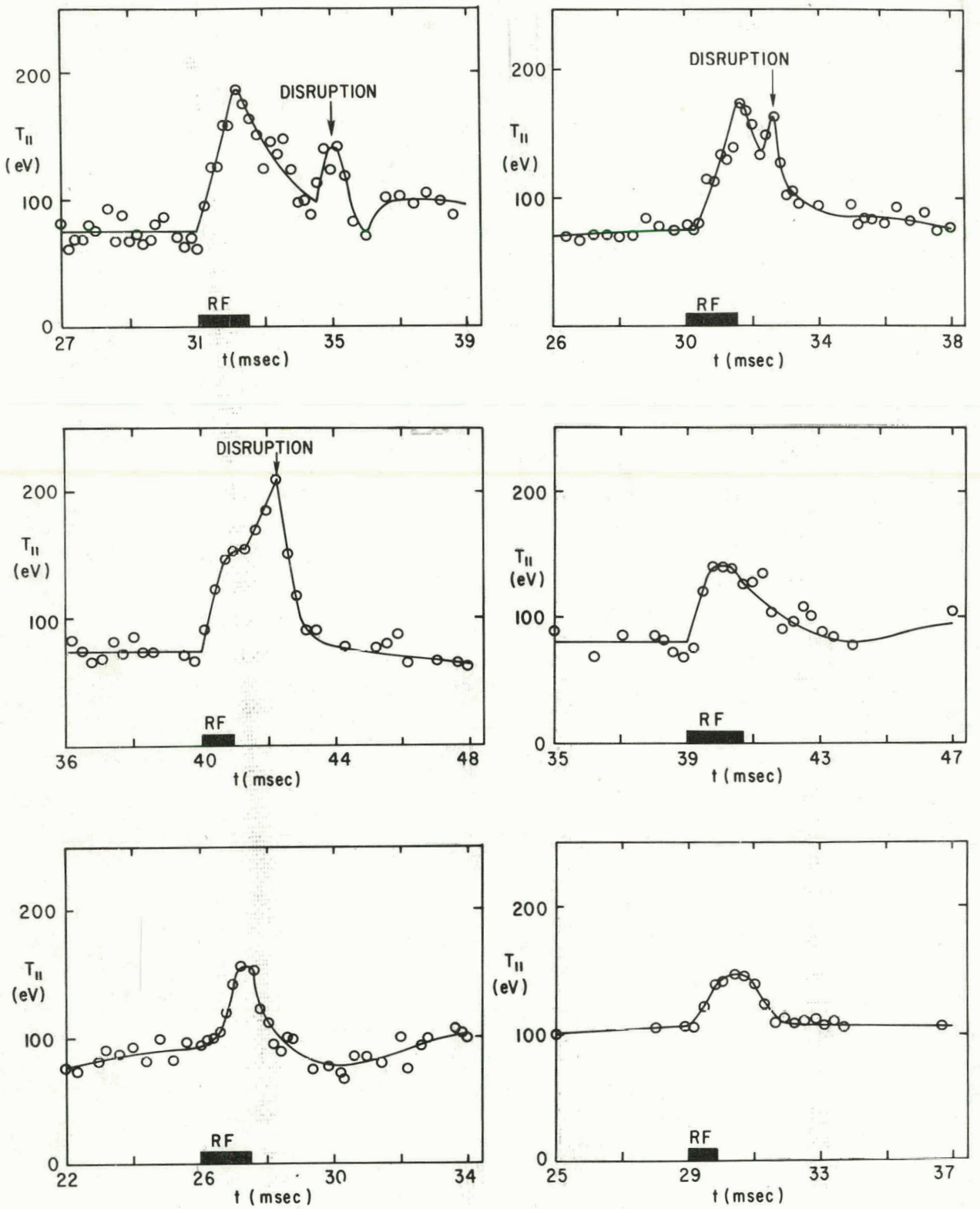

743862

Fig. 6. Some examples of parallel temperature response. In some cases disruption of the plasma due to impurity influx was observed.

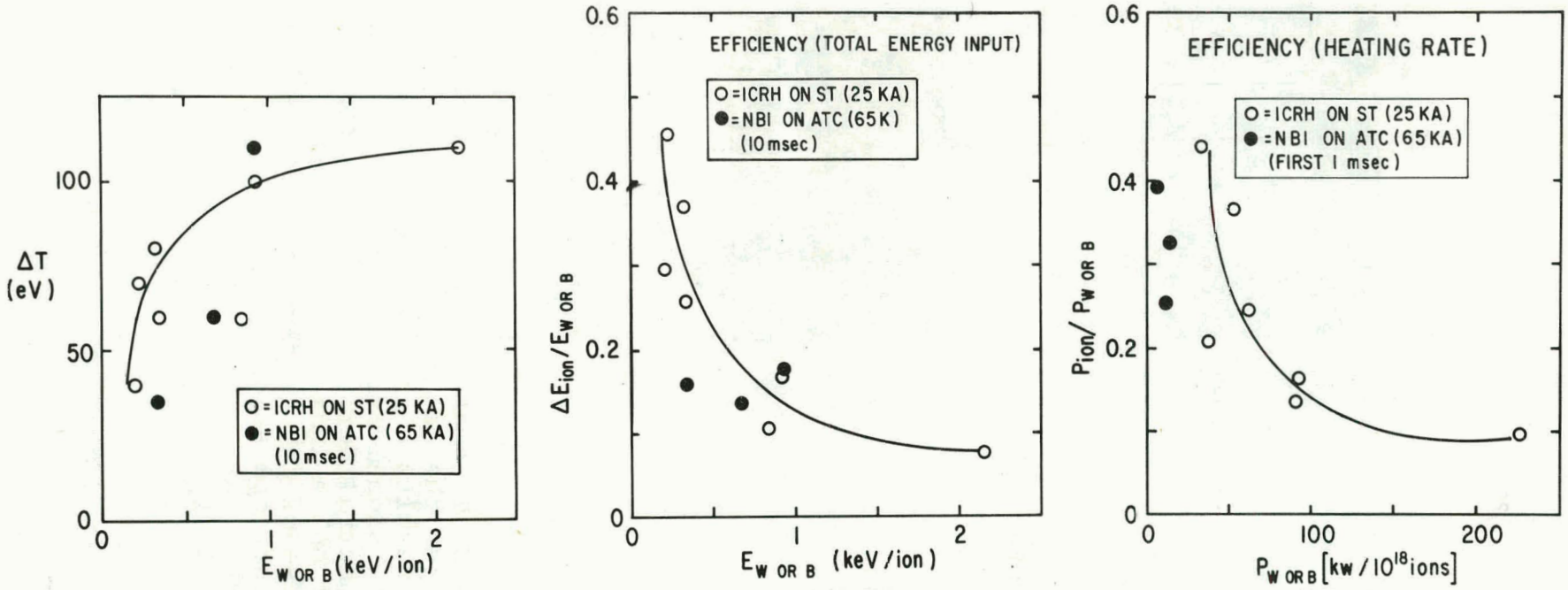

753389

Fig. 7. Incremental temperature increase and efficiencies for ICRH and neutral beam injection heating. For (a) and (b) the abscissa, E_W or $_B$, is the power (of the wave or beam) times pulse length divided by the total number of ions in the machine and represents the amount of energy per ion available for heating. For (b) the beam pulse length of 10 msec over which the temperature increase plotted in (a) was attained is used to compute E_B. ($\Delta E_{ion} = (3/2)k\ \Delta T$). In (c) wave or beam power, P_W or $_B$, is normalized to 10^{18} ions in the machine. P_{ion} is the heating rate, (3/2) k dT/dt. For beam heating the heating rate during the first 1 msec of the pulse is plotted.

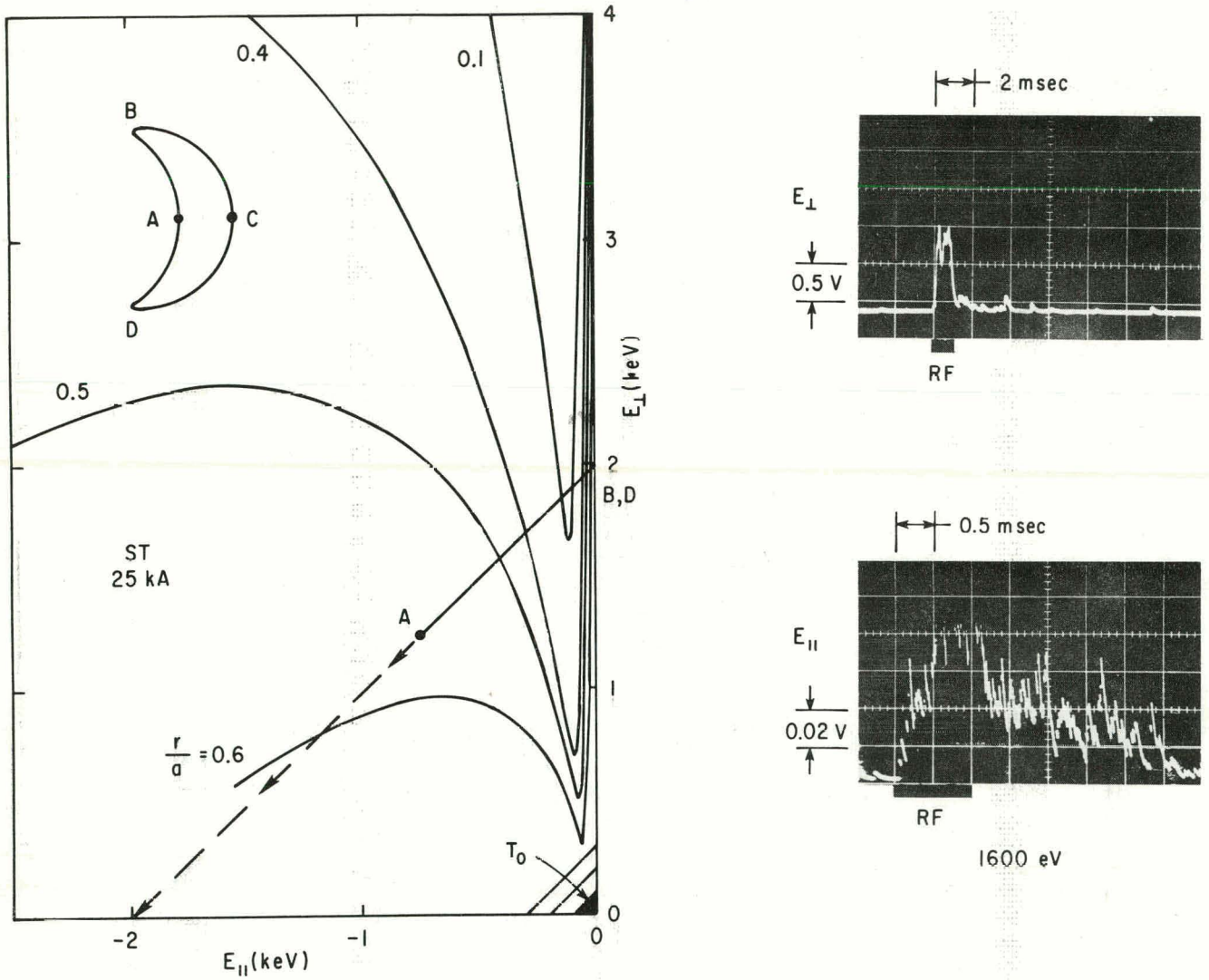

743998

Fig. 8. Loss cones of the ST Tokamak at I_{OH} = 25 kA. (The loss cones are presented after the manner originally due to J. Rome[7], and these specific results were computed by R. Smith.) The oscillograms show signals from perpendicular and tangential charge exchange neutral detectors at E = 1600 eV. Much greater $E_\perp$ signal during rf pulse indicates a strongly anisotropic distribution. Because of intervening loss cones many energetic ions undergoing isotropization via direct deflecting collisions become lost. The $E_\parallel$ signal therefore decreases, rather than increases at the expense of the $E_\perp$ signal, after rf pulse ends.

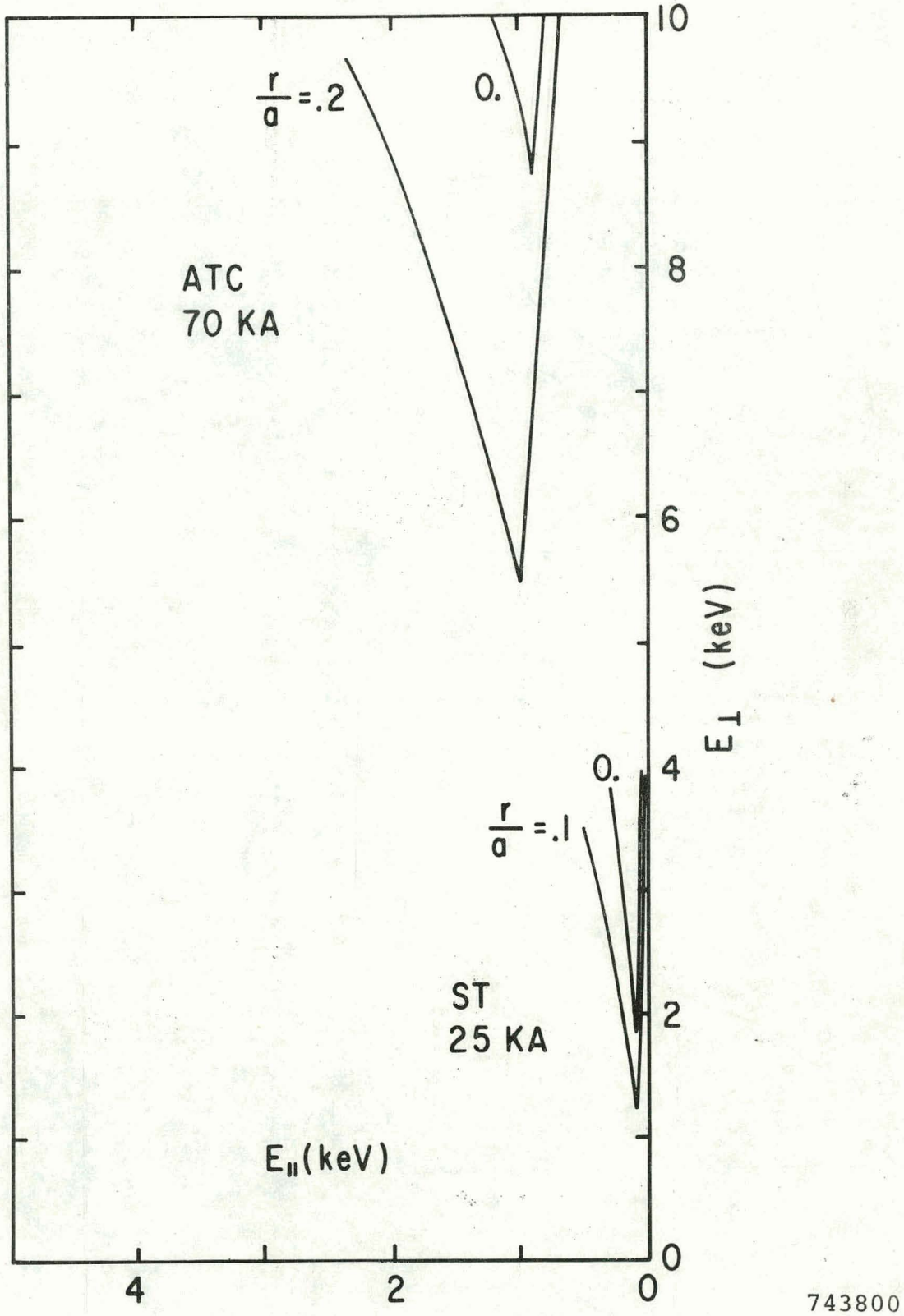

Fig. 9. Comparisons of loss cones of ST at I_{OH} = 25 kA and those of ATC at I_{OH} = 70 kA. (The loss cones are presented after the manner originally due to J. Rome,[7] and the specific results were obtained using a computer code written by R. Smith.)

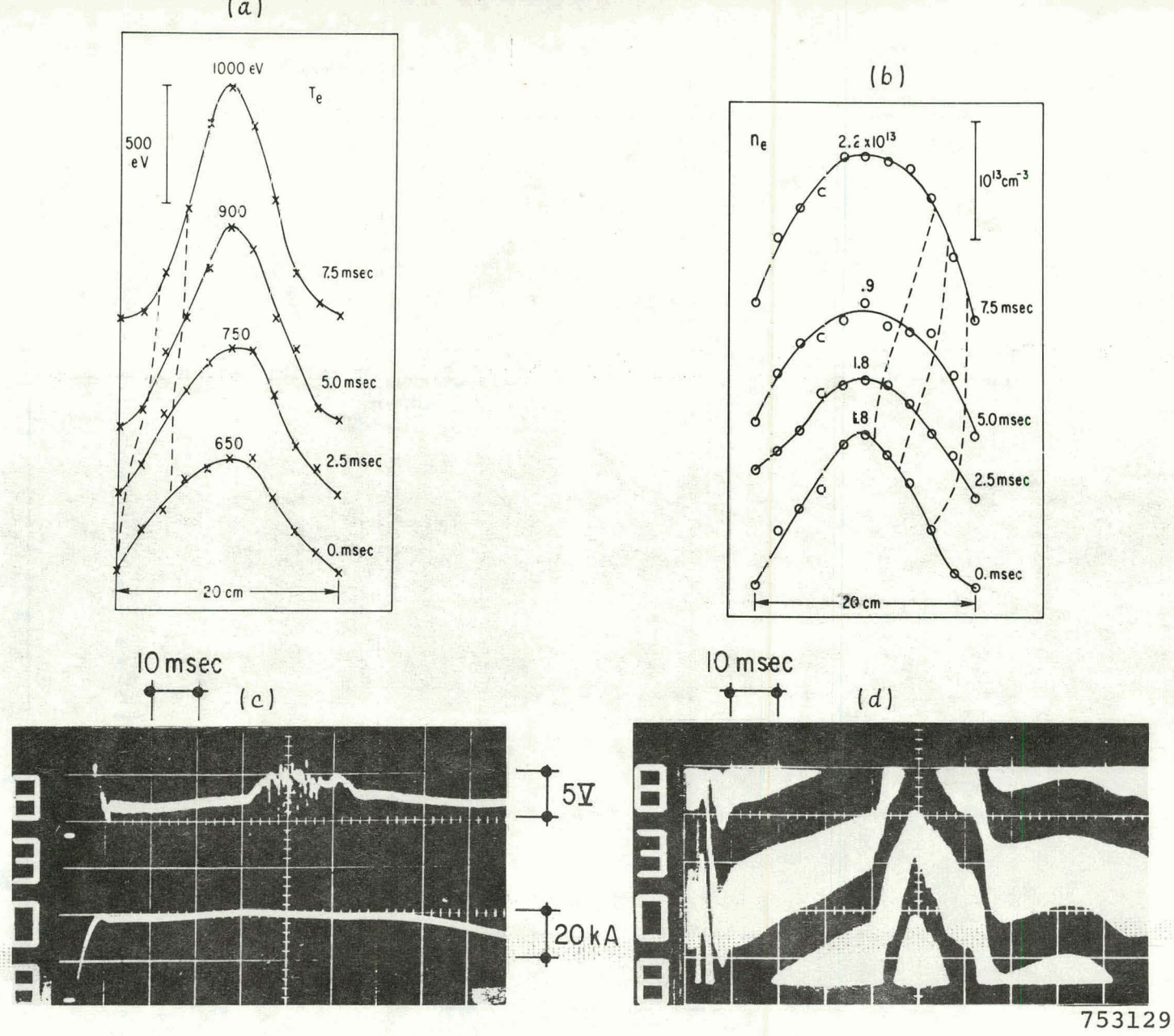

Fig. 10. Sequence of events leading to disruptive instabilities. Variation with time of the radial profile of (a) electron temperature and (b) electron density. Profiles at different times after the initiation of a 10 msec rf pulse are displaced vertically for better visibility, and the dotted lines connect the points of constant T_e or n_e. (c) One-turn loop voltage and Ohmic heating current (d) microwave interferometer trace.

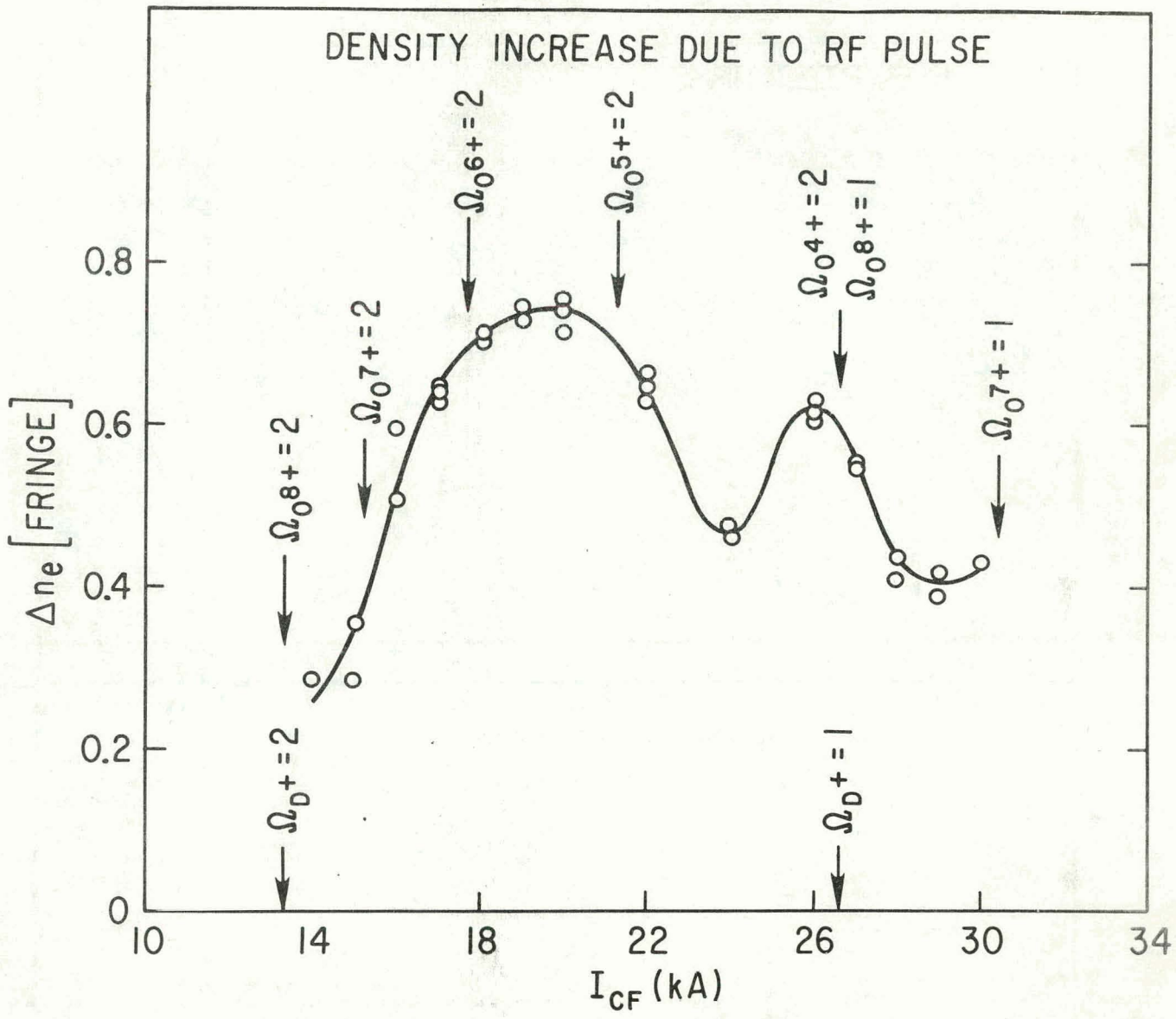

753127

Fig. 11. Density increase due to a 2.5 msec rf pulse as a function of confining field current, I_{CF}. Values of I_{CF} for which the $\Omega = 1$ or $\Omega = 2$ resonant layer for deuterons is located at the center of the plasma are indicated along the abscissa. Resonant conditions for various impurity oxygen ions are indicated along the curves.

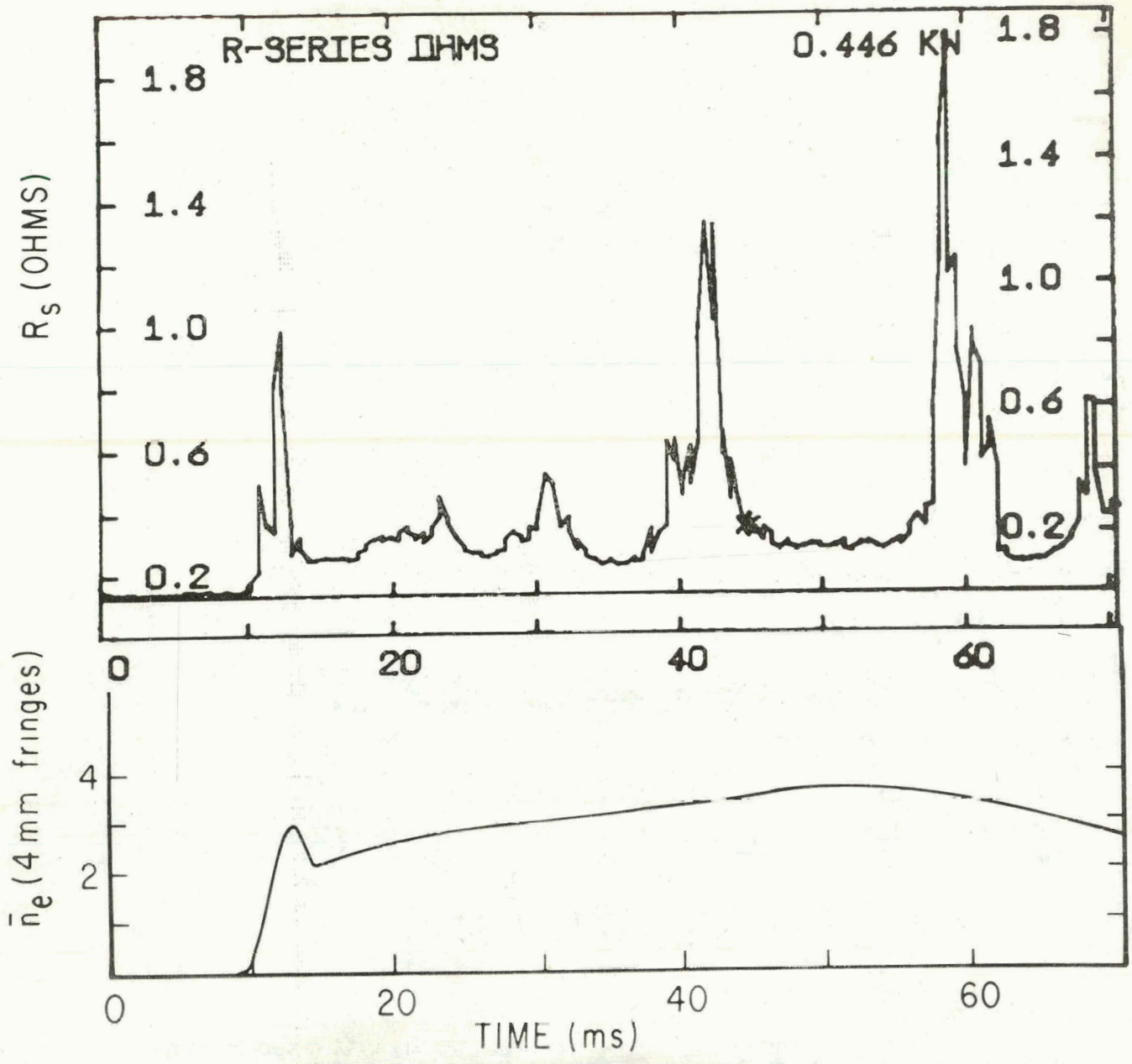

Fig. 12. Loading resistance at $\Omega = 1.16$ and electron density variation with time. Sharp peaks in the loading curves are interpreted as due to toroidal eigenmodes.